

Investigation of the Synthesis of Chitosan Coated Iron Oxide Nanoparticles under Different Experimental Conditions

S. Zeinali^{1, 2, *}, S. Nasirimoghaddam¹ and S. Sabbaghi^{1, 2}

¹Department of Nanochemical Engineering, Faculty of Advanced Technologies, Shiraz University, Shiraz, Iran

²Nanotechnology Research Institute, Shiraz University, Shiraz, Iran

(*) corresponding author: zeinali@shirazu.ac.ir

(Received: 13 January 2014 and Accepted: 10 November 2015)

Abstract

Iron oxide (Fe_3O_4) nanoparticles with average sizes of 10 nm were synthesized by a chemical co-precipitation method in the presence of chitosan. Chitosan as a natural polymer which can be extracted from crustaceans was used in the synthesis process in order to achieve more dispersed nanoparticles. Also, chitosan was used to obtain functionalized magnetic nanoparticles for using in different area of research. Chitosan should be first carboxymethylated and then covalently bounded onto the surface of Fe_3O_4 nanoparticles via carbodiimide activation. Because of size – dependent different property of nanoparticles, The effects of the carboxymethyl chitosan concentration, sonication time and the reaction temperature in the synthesis procedure of chitosan-bound Fe_3O_4 nanoparticles were investigated and then the best condition used for final product. Dynamic light scattering were used to investigate the effect of each experimental parameters on the size and size distribution of prepared nanoparticles. Transmission electron microscopy (TEM), dynamic light scattering (DLS), UV-Vis and FT-IR spectroscopy, vibrational sample magnetometer (VSM) and zeta-potential methods were carried out on the final product in order to characterize the size, size distribution, magnetic property and surface charge of as-prepared nanoparticles.

Keywords: Chitosan, Magnetic nanoparticles, Synthesis.

1. INTRODUCTION

Nanotechnology has emerged at the forefront of science and technology developments. Nanoparticles (NPs) have a wide range of applications in different aspects of human life [1]. superparamagnetic iron oxide nanoparticles especially Fe_3O_4 ferrites magnetic nanoparticles have been rising as a significant useful material due to their specific properties such as superparamagnetism, low toxicity and small size, chemical stability and biocompatibility, etc [2]. Magnetic nanoparticles are used to coat several surfactants to anti – aggregation which was caused by magnetic dipole – dipole

attractions between particles [3–6]. A variety of materials have been reported to modify Fe_3O_4 NPs, such as precious metals [7], silica [8], carbon [9] and biopolymers [10, 11, 12]. Chitosan is a partially acetylated glucosamine biopolymer with many useful features such as hydrophilicity, biocompatibility and biodegradability. In addition, the amino groups on the chitosan can also be used for further functionalization with specific components, such as various drugs, specific binding sites, or other functional groups [13, 14, 15].

The physical and chemical properties of nanoparticles, e.g., the surface energy

density, melting temperature, chemical reactivity, and so on, are obviously different from the bulk counterparts and exhibit a distinctly size-dependent behavior. Such a special characteristic mainly arises from the large surface – to – volume ratio. Surface free energy density is the most importantly physical attribute characterizing the nature of surface effect, which can be interpreted as a reversible work per unit area involved in creating a new surface. For nanoparticles, a strong size effect of surface energy density emerges when the particle diameter is less than a few nanometer. As a result reported from previous work, the surface energy density decreases with the increase of nanoparticle diameter [16].

In this work, Fe₃O₄ magnetic nanoparticles by coprecipitation of Fe(II) and Fe(III) in the presence of ammonia solution were prepared. Since chitosan has no suitable functional groups to bind directly onto Fe₃O₄ nanoparticles, it should be first carboxymethylated and then covalently bound onto Fe₃O₄ nanoparticles via carbodiimide activation. Because the size of Fe₃O₄ magnetic nanoparticles played important roles in different industries such as drug delivery and toxic metal removal. So, in order to property improvement of surface area-to-volume ratio of nanoparticles, effect of some experimental parameters on size and size distribution of chitosan bound Fe₃O₄ nanoparticles to their prospective application in different industries which could be used to synthesize Fe₃O₄ magnetic nanoparticles with different size to meet the requirements of different applications were investigated in this study for the first time.

As will be shown, properties of magnetic nanoparticles could be controlled by adjusting concentration of chitosan, sonication time and reaction temperature during the synthesis. The effect of the above mentioned parameters on the synthesized chitosan bound magnetic nanoparticles were investigated using dynamic light scattering

(DLS) data. At optimal conditions the prepared nanoparticles were characterized by different techniques such as transmission electron microscopy (TEM), FTIR and UV-Vis spectroscopy. Also, Magnetic property and surface charges of nanoparticles were determined using vibrating sample magnetometer (VSM) and zeta-potential measurement.

2. EXPERIMENTAL

2.1. Materials

Chitosan, ferrous chloride tetrahydrate (FeCl₂. 4H₂O), Ferric chloride hexahydrate (FeCl₃. 6H₂O), Ammonium hydroxide (NH₄OH) and monochloroacetic acid (CH₂ClCO₂H) were purchased from Merck and Carbodiimides (cyanamide, CH₂N₂) were purchased from Aldrich. All chemicals were guaranteed or analytic grade reagents commercially available and used without further purification.

2.2. Apparatus

The prepared magnetite nanoparticles were characterized by transmission electron microscopy (TEM– Philips, CM10), Fourier transform infrared spectroscope (FT-IR– Perkin-Elmer, RX1), dynamic light scattering (DLS– HORIBA L-550), vibration sample magnetometer (VSM–Meghnatis Daghighe Kavir(MDK)), UV-Vis spectrophotometer (Shimadzu UV-1800) and zeta-potential analyzer (ZEN 3600, Malvern).

2.3. Preparation of chitosan-bound Fe₃O₄ nanoparticles

Fe₃O₄ nanoparticles were prepared by coprecipitating the Fe³⁺ and Fe²⁺ ions by ammonia solution and treating under hydrothermal conditions [17]. Chemical precipitation was achieved at 25 °C under vigorous stirring by adding NH₄OH solution. The precipitates were heated at 80 °C for 30 min, washed several times with water and

ethanol, and then finally dried in a vacuum oven at 70 °C.

Chitosan was carboxymethylated according to the following method [18]. First, 3 g chitosan and 15 g sodium hydroxide were added into 100 ml of isopropanol/water (80/20) mixture at 60 °C to swell and alkalize for 1 h. Then, 20 ml of monochloroacetic acid solution (0.75 gml⁻¹ in isopropanol) was added into the reaction mixture in drops in 30 min. After reaction for 4 h at the same temperature, 200 ml of ethyl alcohol was added to stop the reaction. Finally, the solid was filtered, rinsed with ethyl alcohol to desalt and dewater, and dried in an oven at 50 °C.

The binding of carboxymethyl chitosan (CM-chitosan) was conducted to bind on magnetic nanoparticles. First, 100 mg of Fe₃O₄ nanoparticles was added to 2 ml of buffer A (0.003 M phosphate, pH 6, 0.1 M NaCl). Then, the reaction mixture was sonicated for 10 min after adding 0.5 ml of carbodiimide solution (0.025 gml⁻¹ in buffer A). Finally, 2.5 ml of carboxymethyl chitosan solution (50 mg ml⁻¹ in buffer A) was added and the reaction mixture was sonicated for 60 min. The chitosan-bound Fe₃O₄ nanoparticles were recovered from the reaction mixture by placing the bottle on a permanent magnet with a surface magnetization of 4000 G. The magnetic particles settled within 1–2 min and then were washed with water and ethanol.

3. RESULTS AND DISCUSSION

The uncoated Fe₃O₄ nanoparticles were synthesized by hydrothermal condition, then the carboxymethylated chitosan, previously prepared, was used for coating of Fe₃O₄ nanoparticles surfaces. Different conditions such as, various temperature, sonication time and concentration of the chitosan were

changed during the experiments. It is considerable that these parameters have important effects on the characteristics of products. The particle size in crystallization is controlled mainly through the rate processes of nucleation and grain growth, which compete for the species. Their rates depend upon the reaction temperature, with other conditions held constant. Nucleation might be faster than grain growth at higher temperatures and results in a decrease in particle size. On the other hand, prolonging the reaction time would favor grain growth. The DLS experiment was conducted with a (HORIBA L-550) at a fixed scattering angle of 90° and at a constant temperature of 25°C.

3.1. Effect of concentration of CM-chitosan

Different concentrations of carboxymethyl chitosan (10 mg/ml, 30 mg/ml, 50 mg/ml) were used for preparing magnetic nanoparticles. In this way, all other parameters kept constant (room temperature and 60 min sonication time) and the effect of the concentration variation of chitosan was investigated on the size of Fe₃O₄ nanoparticles. The DLS graphs by varying chitosan concentrations were shown in Figure 1. The average particle sizes of the nanoparticles prepared using 10 mg/ml, 30 mg/ml and 50 mg/ml of chitosan are 12.7, 9.1 and 7.7 nm, respectively.

The results evidence that the size of nanoparticles become smaller by increasing the chitosan concentration due to better protecting the nanoparticles' surface from aggregation. By increasing the chitosan concentrations more than 50 mg/ml no remarkable changes in size was observed. So, in order to consuming less chitosan, 50 mg/ml was chosen as the best value for future experiments.

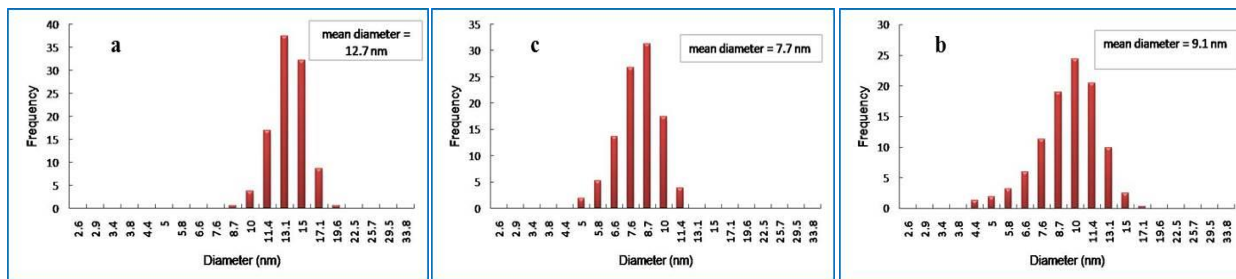


Figure 1. DLS graphs for preparation of chitosan-bound Fe_3O_4 nanoparticles at chitosan concentration of (a) 10 mg/ml (b) 30 mg/ml and (c) 50 mg/ml, respectively.

3.2. Effect of sonication time

One of other important parameters can be influence on the size and size distribution of nanoparticle is the sonication time. An effective sonication process can inhibit the agglomeration of the nanoparticle efficiently. So, the sonication times were changing by 30, 45, 60 min in last step of the synthesis. It is notable that these experiments were done at the optimum concentration of chitosan reported in the previous section. The results were presented in Figure 2. The

average particle sizes of chitosan coated Fe_3O_4 prepared at sonication times of 30, 45 and 60 min are 13.7 nm, 9.6 nm and 7.7 nm, respectively. As expectable, increasing the sonication time results in decreasing the nanoparticles size due to sufficient deagglomeration. At very high sonication time, the separation of chitosan coating from the nanoparticle surfaces may be occurred, so 60 min were considered as the best.

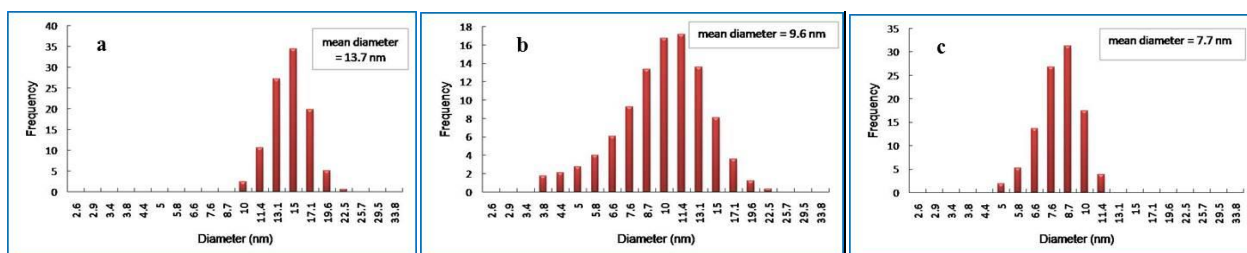


Figure 2. DLS graphs for preparation of chitosan-bound Fe_3O_4 nanoparticles at sonication time of (a) 30 min (b) 45 min and (c) 60 min, respectively.

3.3. Effect of reaction temperature

A series of controllable experiments were carried out at different temperature, at obtained optimal values for chitosan and the sonication time previously, to investigate the effect of the reaction temperature on the size of nanoparticles. Figure 3 shows the DLS graphs of the samples obtained at different reaction temperature. As shown, the average particle sizes of chitosan- Fe_3O_4

nanoparticles prepared at 25 °C, 50 °C and 80 °C are 7.7 nm, 6.6 nm and 3.2 nm, respectively. It is found that with increasing temperature, the size of nanoparticles decreased. This confirmed that at high temperatures nucleation rate overcome than growth rate. Although, working at room temperature is more economically and it is preferred to prepare nanoparticles at ambient conditions.

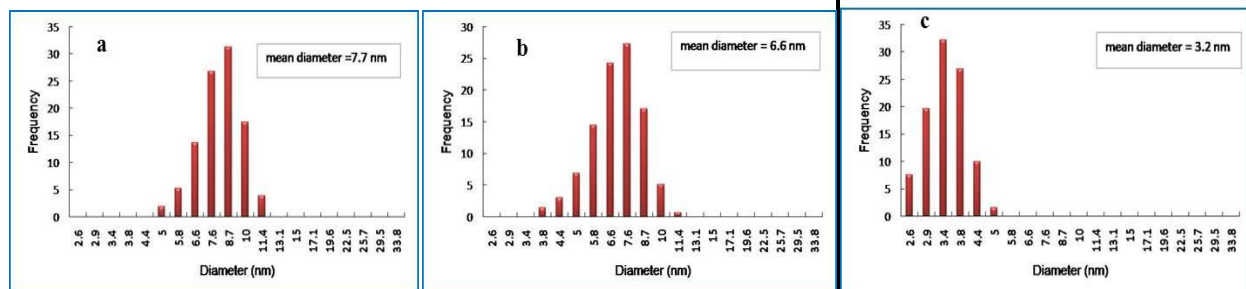


Figure 3. DLS graphs for preparation of chitosan-bound Fe_3O_4 nanoparticles at reaction temperatures of (a) 25 °C (b) 50 °C and 80 °C, respectively.

Finally, the chitosan-bound Fe_3O_4 nanoparticles prepared at optimum conditions (25 °C, 60 min sonication time and 50 mg/ml) were characterized using different techniques. Transmission electron microscopy (TEM), dynamic light scattering (DLS), UV-Visible spectrophotometry, Fourier transform infrared spectroscopy (FT-IR) were used to identifying the size and shape of nanoparticles. The magnetic properties and surface charges were studied using vibration sample magnetometer (VSM) and Zeta-potential analyzer.

3.4. Characterizations of chitosan-bound Fe_3O_4 nanoparticles

3.4.1. Transmission electron microscopy (TEM)

TEM micrographs of the colloidal dispersions were obtained by a transmission electron microscope operated at an accelerating voltage of 100kV. The typical TEM micrographs for the chitosan-bound Fe_3O_4 nanoparticles are shown in Figure 4. It was clear that the chitosan can inhibit the aggregation of nanoparticles so, chitosan-bound Fe_3O_4 nanoparticles had essentially low dispersion with a mean diameter of about 7.7 nm compared to the naked nanoparticles (about 10 nm). This could be attributed to the reaction occurring only on the particle surface, and thus our attempt to prepare monodispersed chitosan-bound Fe_3O_4 nanoparticles in this work has been achieved.

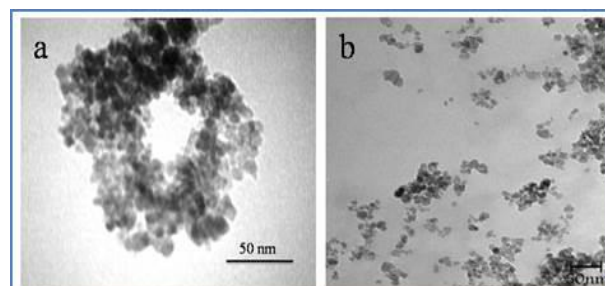


Figure 4. TEM micrographs for (a) naked and (b) chitosan-bound Fe_3O_4 nanoparticles.

3.4.2. Dynamic Light Scattering

The DLS experiment was conducted at a constant temperature of 25°C. Figure 5 shows the size distribution graphs for the naked and chitosan-bound Fe_3O_4 nanoparticles obtained by DLS method according to size distribution data analysis. These reveal that range of distribution of the resultant nanoparticles were narrow. This also confirms the binding of chitosan on Fe_3O_4 nanoparticles that leads to lowering their size.

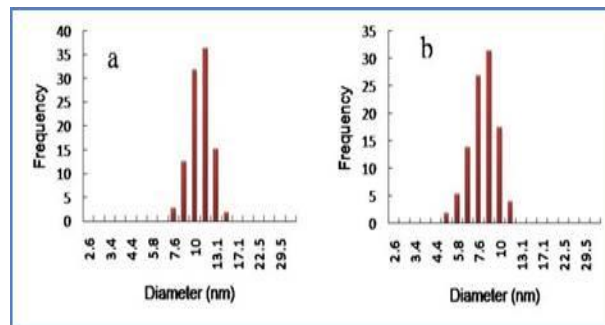


Figure 5. DLS graphs for (a) naked and (b) chitosan-bound Fe_3O_4 nanoparticles.

3.4.3. UV-Vis Spectrophotometry

UV-Vis spectra of the magnetic nanoparticles were recorded by using a 1-cm quartz cell. Figure 6 shows the absorption spectra of naked and chitosan coated magnetic nanoparticles which their differences can be considered as another evidence for binding of chitosan on the magnetic nanoparticles surfaces.

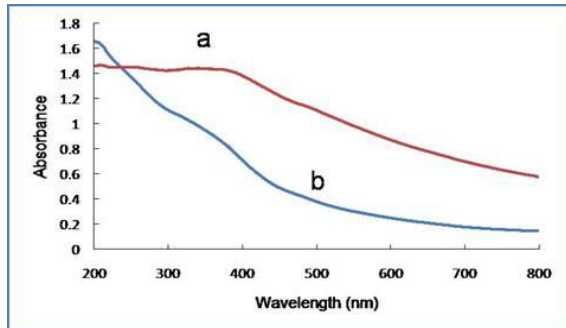


Figure 6. The absorption spectra of (a) naked and (b) chitosan coated Fe_3O_4 nanoparticles.

3.4.4. FT-IR spectroscopy

To confirm the existence of the surface coating, naked Fe_3O_4 (a), chitosan (b) and chitosan bounded Fe_3O_4 (c) nanoparticles were characterized using FTIR spectroscopy and the results have been shown in Figure 7. The prepared disks were used to get the FTIR results. By comparison of the FTIR spectra (“a”, “b” and “c” spectra in Figure 7), the presence of the chitosan coating changed the FTIR pattern of Fe_3O_4 significantly. In spectrum “a”, the peak at 585cm^{-1} corresponds to the Fe–O bond vibrating of Fe_3O_4 that shifted to about 590 for chitosan bounded Fe_3O_4 . In spectrum “b”, the peak at 3406cm^{-1} is attributed to O–H stretching vibrations. The peak at 2860cm^{-1} are attributed to the of C–H stretching vibration of the polymer backbone. Besides, the stretch vibration of C–O is found at 1078 and 1034cm^{-1} . The adsorption bands around 3406 and 1611cm^{-1} observed in two spectra are attributed to the deformation vibration of N–H in primary amine ($-\text{NH}_2$). As can be

seen in spectrum “c”, the IR spectra indicated that chitosan and Fe_3O_4 special peaks are both presented in magnetic chitosan nanoparticles, so it can concluded that the Fe_3O_4 magnetic nanoparticles were effectively coated by the chitosan.

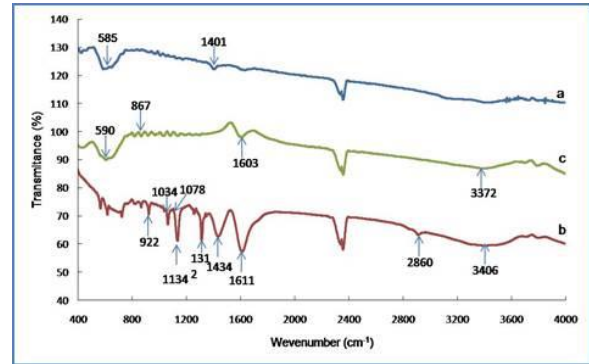


Figure 7. FTIR spectra of (a) naked Fe_3O_4 (b) CM-chitosan, and (c) CM-chitosan coated Fe_3O_4 nanoparticles.

3.4.5. Vibration sample magnetometer (VSM)

The magnetic properties of both uncoated and coated Fe_3O_4 nanoparticles were measured with a vibrating sample magnetometer (VSM) at room temperature. Figure 8 shows a typical magnetization curve of naked Fe_3O_4 nanoparticles and chitosan-bound Fe_3O_4 nanoparticles. As could be seen from Figure 8, the hysteresis loop shows superparamagnetic property, indicating that the single-domain magnetic nanoparticles remained in these nanoparticles. The saturation magnetization (Ms) of the naked Fe_3O_4 nanoparticles was about 54emu/g , while for chitosan-bound Fe_3O_4 nanoparticles was about 50emu/g in this experiment. Because the same amounts of all used nanoparticles for this experiment, it can be concluded that the decrease of saturation magnetization is due to the presence of chitosan. The existence of chitosan on the surface of Fe_3O_4 nanoparticles has decreased the uniformity due to quenching of surface moments, resulting in the reduction of magnetic

moment in such nanoparticles. This value was considerably higher than that of other reported chitosan based Fe_3O_4 beads [48–50]. Therefore, our chitosan coated magnetic nanoparticles can be easily separated by applying the external magnetic field.

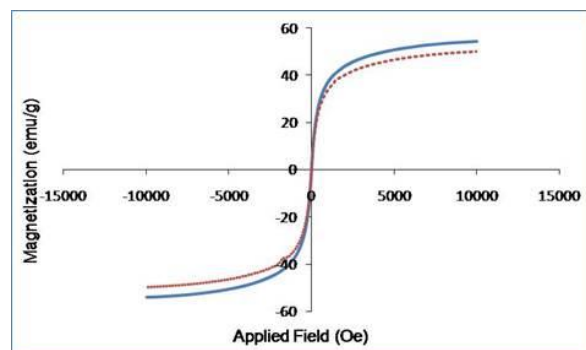


Figure 8. Magnetic hysteresis curves of naked (solid line) and chitosan coated (dot line) Fe_3O_4 nanoparticles.

3.4.6. Zeta-potential analysis

Zeta potential analyzer (ZEN 3600, Malvern Co.) was performed to investigate the surface net charge of nanoparticles. Zeta potential values of chitosan bound Fe_3O_4 nanoparticles dispersed at universal buffer solutions (acidic (pH 3) and basic (pH 9)) were measured. The results (Figure 9) show negative values for basic and positive value at acidic media as it is expectable (according to the isoelectric point of chitosan = 5). These results are expectable because of the amine, carboxylic and hydroxyl groups of chitosan.

4. CONCLUSION

Magnetic Fe_3O_4 -chitosan nanoparticles were fabricated by the covalent binding of

REFERENCES

1. Zhang, L., Webster, T. J., (2009). "Nanotechnology and nanomaterials: Promises for improved tissue regeneration", *Nano Today*, 4: 66–80.
2. Khayat Sarkar, Z., Khayat Sarkar F., (2013). "Selective Removal of Lead (II) Ion from Wastewater Using Superparamagnetic Monodispersed Iron Oxide (Fe_3O_4) Nanoparticles as a Effective Adsorbent", *Int. J. Nanosci. Nanotechnol.*, 9: 109-114.
3. Faraji, M., Yamini, Y., Rezaee, M., (2010). "Magnetic nanoparticles: Synthesis, stabilization, functionalization, characterization, and applications", *J. Iran. Chem. Soc.*, 7: 1–37.

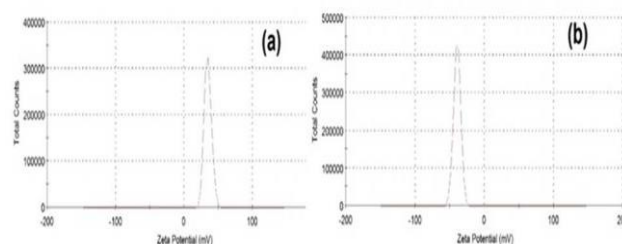


Figure 9. Zeta potential distribution graphs of CM-chitosan coated Fe_3O_4 nanoparticles at (a) pH 3 (b) pH 9.

carboxymethylated chitosan on the Fe_3O_4 nanoparticles. Effects of some parameters such as concentration of CM-chitosan, sonication time and reaction temperature on the nanoparticles size were studied. The results showed all these parameters could influenced on the size of nanoparticles. Due to the good biocompatibility of chitosan, these particles may be used in magnetic-field assisted drug delivery, enzyme or cell immobilization and many other industrial applications. Also his magnetic chitosan nanoparticles have a good potential to remove toxic metal ions which are the problem of drinking water in many of the developed countries.

ACKNOWLEDGMENT

We acknowledge the nanotechnology research Institute of Shiraz University, the ministry of science and technology as providers of financial sum, facilities, and contributors. Also acknowledge Iranian society of nanotechnology for supporting the nano-research in Iran.

4. Zhao, F., Zhang, B., Feng, L., (2012). "Preparation and magnetic properties of magnetite nanoparticles", *Mater. Lett.*, 68: 112–114.
5. Xu, P., Zeng, G. M., Huang, D. L., Feng, C. L., Hu, S., Zhao, M. H., Lai, C., Wei, Z., Huang, C., Xie, G. X., Liu, Z. F., (2012). "Use of iron oxide nanomaterials in wastewater treatment: a review", *Sci. Total Environ.*, 424: 1–10.
6. Li, G.Y., Jiang, Y.R., Huang, K. I., Ding, P., Chen, J., (2008). "Preparation and properties of magnetic Fe₃O₄ – chitosan nanoparticles", *J. Alloys Compd.*, 466: 451–456.
7. Wang, L. Y., Park, H. Y., Lim, S. I. I., Schadt, M. J., Mott, D., Luo, J., Wang, X., Zhong, C. J., (2008). "Core@shell nanomaterials: gold-coated magnetic oxide nanoparticles", *J. Mater. Chem.*, 18: 2629–2635.
8. Stjern Dahl, M., Andersson, M., Hall, H. E., Pajeroski, D. M., Meisel, M. W., Duran, R. S., (2008). "Superparamagnetic Fe₃O₄ /SiO₂ nanocomposites: enabling the tuning of both the iron oxide load and the size of the nanoparticles", *Langmuir*, 24: 3532–3536.
9. Xu, L. Q., Zhang, W. Q., Ding, Y. W., Peng, Y. Y., Zhang, S. Y., Yu, W. C., Qian, Y. T., (2004). "Formation, characterization, and magnetic properties of Fe₃O₄ Nanowires encapsulated in carbon microtubes", *J. Phys. Chem. B*, 108: 10859–10862.
10. Ren, J., Hong, H.Y., Ren, T. B., Teng X. R., (2006). "Preparation and characterization of magnetic PLA-PEG composite nanoparticles for drug targeting", *React. Funct. Polym.*, 66: 944–951.
11. Zhang, Y., Zhang, J., (2005). "Surface Modification of Monodisperse Magnetite Nanoparticles for Improved Intracellular Uptake to Breast Cancer Cells", *J. Colloid Interface Sci.*, 283: 352–357.
12. Laurent, S., Forge, D., Port, M., Roch, A., Robic, C., Elst, L. V., Muller, R. N., (2008). "Magnetic iron oxide nanoparticles: synthesis, stabilization, vectorization, physicochemical characterizations, and biological applications", *Chem. Rev.*, 108: 2064–2110.
13. Wan Ngaha, W. S., Teong, L. C., Hanafiah, M. A. K. M., (2011). "Adsorption of dyes and heavy metal ions by chitosan composites: A review", *carbohydrate Polym.*, 83: 1446–1456.
14. Ravi Kumar, M. N. V., (2000). "A review of chitin and chitosan applications", *React. Funct. Polym.*, 46: 1–27.
15. Ghaee1, A., Shariaty-Niassar, M., Barzin, J., Ismail, A. F., (2013). "Chitosan/Polyethersulfone Composite Nanofiltration Membrane for Industrial Wastewater Treatment", *Int. J. Nanosci. Nanotechnol.*, 9: 213–220.
16. Khayat Sarkar, Z., Khayat Sarkar, F., (2011). "Synthesis and Magnetic Properties Investigations of Fe₃O₄ Nanoparticles" *Int. J. Nanosci. Nanotechnol.*, 7: 197–200.
17. Mohapatra, S., Pal, D., Ghosh, S. K., Pramanik, P., (2007). "Design of superparamagnetic iron oxide nanoparticle for purification of recombinant proteins", *J. Nanosci. Nanotechnol.*, 7: 3193–3199.
18. Sun, G. , Chen, X. , Li, Y. , Zheng, B. , Gong, Z. , Sun, J. , Chen, H. , Li, J. , Lin, W. (2008). "Preparation of H-oleoyl-carboxymethyl-chitosan and the function as a coagulation agent for residual oil in aqueous system", *Front. Mater. Sci. China.*, 2: 105–112.